Desalination and Water Treatment
www.deswater.com
doi: 10.5004/dwt.2018.22417

118 (2018) 61–69
June

Inter-tube flow characteristics of horizontal tube falling film

X. Chen[a], L.Y. Gong[b], S.Q. Shen[b,*], T. Lu[a]

[a]*School of Mechanical and Electrical, Beijing University of Chemical Technology, Beijing 100029, China, emails: xchen@buct.edu.cn (X. Chen), likesurge@sina.com (T. Lu)*
[b]*School of Energy and Power Engineering, Dalian University of Technology, Dalian 116024, China, Tel. +86 0411 84708464; emails: zzbshen@dlut.edu.cn (S.Q. Shen), dutgly@yahoo.com (L.Y. Gong)*

Received 27 November 2017; Accepted 22 April 2018

ABSTRACT

Inter-tube flow pattern of horizontal tube falling film dominates the flow state of thin film around the tube and influences heat transfer. An observation experiment was performed to investigate the inter-tube flow characteristics of horizontal tube falling film focusing on 19 and 25.4 mm-diameter Al-brass tubes with the Reynolds number ranging from 64.4 to 598. The flow pattern images were captured by a high-definition camera and a high-speed camera with backlight method. Flow patterns were characterized and their transitions were classified. Phenomena occurred in flow pattern transition were discussed with the variation of Reynolds number, tube spacing, and tube diameter. The results show that the critical transition Reynolds number increases with tube spacing. Special flow patterns were observed and classified when the tube spacing was undersize. The hysteresis in horizontal tube falling film flow were discussed in detailed.

Keywords: Horizontal tube falling film; Flow pattern; Critical transition Reynolds; Hysteresis phenomenon

1. Introduction

Horizontal tube falling film evaporation has been widely used in desalination plants, refrigeration, chemical engineering, and food processing due to high heat transfer rate and low temperature difference [1]. Horizontal tube falling film flow can be divided into inter-tube flow and thin film flow around a tube according to liquid location. Many studies investigated the flow state of thin liquid film outside horizontal tubes [2–5], but the studies are relatively fewer for the inter-tube flow pattern of horizontal tube falling film. In horizontal tube falling film evaporator, the inter-tube flow determines the way, the intense, and the scope of impingement on tube surface, which all affect the convection heat transfer by affecting the film fluctuation [6–8]. Hence, the inter-tube flow pattern, as a significant aspect of horizontal tube falling film flow, is worthy of concern and study.

With the increment of spray density, the inter-tube flow patterns of horizontal tube falling film under conventional scale tube spacing are normally divided into three idealized flow patterns in sequence: droplet flow, column flow (or jet flow), and sheet flow, as shown in Fig. 1. Yung et al. [9] studied droplet flow and column flow of horizontal tube falling film, correlated the spray density for the transition from the droplet pattern to the column pattern by making the droplet production frequency set equal to the capillary wave oscillation frequency. Armbruster and Mitrovic [10] found that the column flow can be classified into inline flow and staggered flow according to the detach location of the lower liquid column. Based on previous researches, Hu and Jacobi [11] presented more detailed flow modes: droplet pattern, droplet-column pattern, inline column pattern, staggered column pattern, column-sheet pattern, and sheet pattern. Fujita and Tsutsui [12] defined two flow patterns: the distinct droplet pattern and the disturbed columns pattern. The former refers to that the liquid initially falls as a column and then

* Corresponding author.

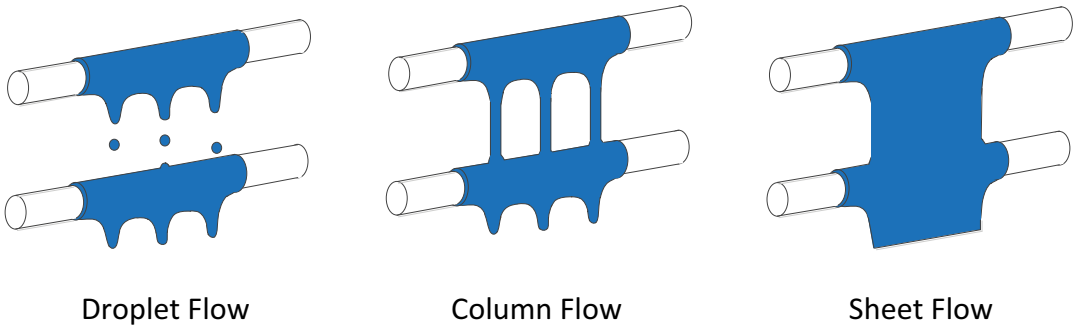

Fig. 1. Idealized flow patterns.

disintegrates into droplets due to the increase of the falling velocity; the latter refers to the liquid columns which may combine with a neighbor column and results in an instable sheet, then ruptures.

Conclusions on flow pattern transition have not been identical. Ganić and Roppo [13] pointed out that the transition from droplet flow to column flow occurs at Re = 150–200, and is affected by the tube spacing. Mitrovic [7] also suggested that the tube spacing can influence flow pattern transition. A similar result was obtained by Killion and Garimella [14,15] when they observed the droplet flow of LiBr by using a high-speed camera. On the contrary, Armbruster and Mitrovic [10] deemed that the flow pattern transition is only dependent on flow rate. Hu and Jacobi [11], Roques et al. [16] indicated that the flow pattern is almost independent of tube geometric according to their respective experiments. A three-dimensional simulation was performed to investigate the flow pattern transition for 14 mm tube diameter and 14 mm tube spacing by Chen et al. [17]. They proposed that the critical pattern transition flow rate from droplet to column flow is 0.0125 kg/s, and 0.02 kg/s from column to sheet flow. Li et al. [5] also conducted a three-dimensional simulation to investigate the critical pattern transition Reynolds number for 16 mm diameter and 15 mm tube spacing in quiescent surrounding and countercurrent gas flow.

That the critical pattern transition Reynolds numbers when increasing the spray density are usually larger than that when decreasing the spray density is called the hysteresis phenomenon. Dhir et al. [18], Armbruster and Mitrovic [10] pointed out that the hysteresis phenomenon exists in the transition process from column flow to sheet flow. But Hu and Jacobi [11], Ruan et al. [19] found that the hysteresis phenomenon exists in all flow pattern transitions.

Based on the earlier literature survey, the previous studies are relatively limited in flow patterns of horizontal tube falling film. The objective of this paper is to conduct further study on transition mechanism, hysteresis phenomenon, and flow details.

2. Experimental apparatus

Fig. 2 shows the experimental circulation system. The fluid flows out from the upper tank, and then goes through the valve and flowmeter before entering the spray tube. A uniform liquid falling film forms outside the test tubes. At last, the fluid is collected by the storage tank and pumped back to upper tank by the low-noise pump.

The upper tank was designed with a fixed water level to produce steady flow rate. Four Al-brass tubes with the length of 500 mm were fixed horizontally in the adjustable bracket. The top one is the spray tube with 3 mm diameter holes drilled at an interval of 8 mm along the bottom line. The second tube with 2 mm tube spacing from the top tube is the distribution tube. The narrow gap helps the distribution tube to get wetted perfectly and guarantees the uniform falling film. The third and fourth tubes are test tubes with the tube spacings and diameters presented in Table 1.

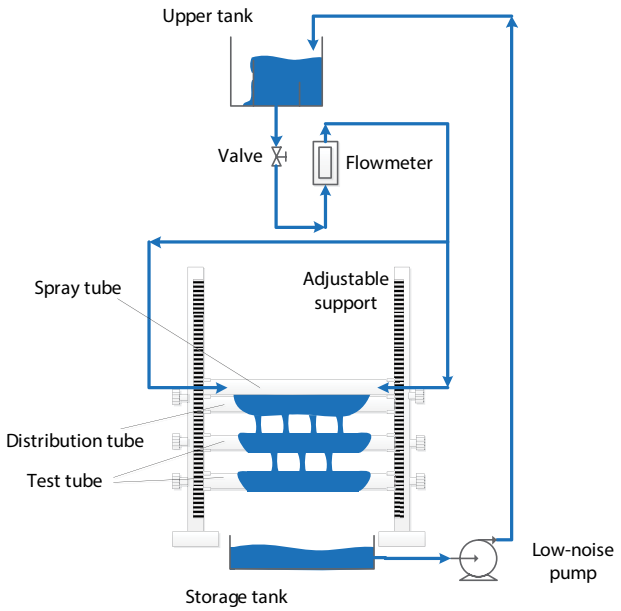

Fig. 2. Schematic of circulation system.

Table 1
Tube diameter and tube spacing

Tube diameter (mm)	Tube spacing (mm)					
19	5.7	10	15.2	20	23.8	30
25.4	–	10	–	20	–	30

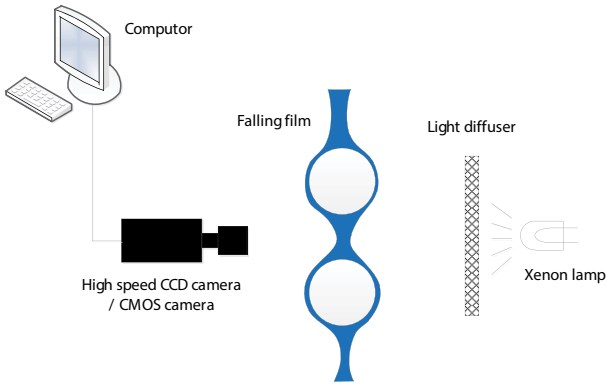

Fig. 3. Schematic of image acquisition system.

The surfaces of all tubes were cleaned carefully before the experiment.

The backlight method was applied for capturing the gas/liquid interface clearly as shown in Fig. 3. The light diffuser helped to generate uniform and soft light from the xenon lamp. A high-definition camera, Cannon 7D with EF 24–70mm f/2.8L lens, was used to take the images as the main camera. Besides, a high-speed camera, Phantom V12.1, with Tokina 100 mm f/2.8 lens was used as the assistant camera to capture the instant images.

The errors of the critical transition Reynolds numbers (Re_c) were evaluated by the measuring error and random error. The error of the flowmeter is 1.5%. A series of actions were taken to minimize the subjective measuring error: (1) only one observer; (2) more than 200 images were taken for each flow rate and more than six observations were performed for each transition; (3) the comprehensive judgments were made based on both high-definition camera and high-speed camera; (4) data were recorded only when flow patterns exist steadily for more than 2 s.

3. Description for terminologies and definitions

3.1. Terminologies

For a better understanding of the flow state description, the terms are shown in Fig. 4 and explained as follows:

- Liquid neck: the slender liquid dragged by the gravity connects droplet to root under droplet flow.
- Main droplet: the droplet which forms at the end of liquid neck under droplet flow.
- Secondary droplet: the droplet forms at the end of liquid neck after the main droplet falls off. The secondary droplet sometimes falls off from the liquid neck following the main droplet closely or sometimes retracts with liquid neck.
- Satellite droplet: the droplets split from liquid neck when it retracts.
- Liquid arch: the fluid which connects a sheet to an adjacent column or sheet.

3.2. Definitions

The spray Reynolds number is defined as follows:

$$\mathrm{Re} = \frac{4\Gamma}{\mu} \tag{1}$$

Spray density Γ refers to the flow rate per length per side and μ refers to the liquid viscosity. From Eq. (1), it indicates that when the thermal properties are constant, the Re is proportional to the spray density.

According to the definition of Roques et al. [16], the inter-tube flow patterns generally display successively as droplet flow, droplet-column flow, column flow, column-sheet flow, and sheet flow. The more detailed definitions are shown as following:

- Droplet flow: the droplet is the only flow pattern between the tubes, as shown in Fig. 5(a);
- Droplet-column flow: this pattern is the transitional form between droplet flow and column flow. There is at least one stable liquid column in this pattern, as shown in Fig. 5(b);
- Column flow: the column is the only flow pattern, as shown in Figs. 5(c) and (d);
- Column-sheet flow: this pattern is the transitional form between column flow and sheet flow. Both liquid sheets and columns exist in this pattern, as shown in Fig. 5(e);
- Sheet flow: the sheet is the only flow pattern. The liquid sheet could be consecutive or inconsecutive, as shown in Fig. 5(f).

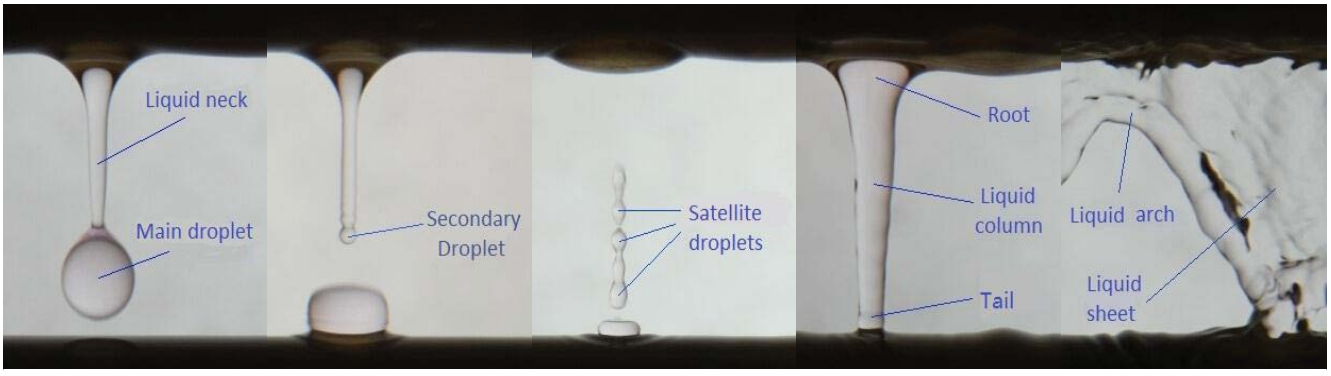

Fig. 4. Terms of the inter-tube flow pattern.

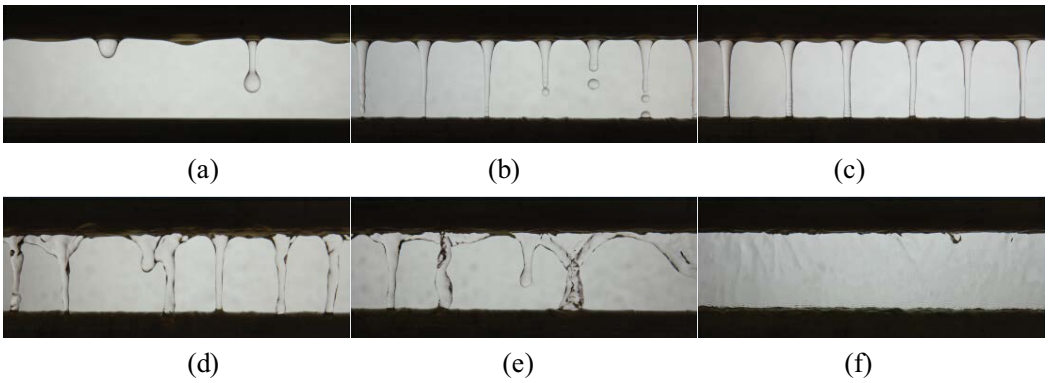

Fig. 5. Classification of flow patterns. (a) droplet flow, (b) droplet-column flow, (c, d) column flow, (e) column-sheet flow, and (f) sheet flow.

4. Results and discussion

4.1. Effect of spray density

4.1.1. Flow pattern

Taking the inter-tube flow when d = 19 mm, s = 30 mm as an example, the flow typically manifests as the following phenomenon:

- Droplet flow

When Re is relatively small, the droplet pattern between adjacent tubes is shown in Figs. 6(a) and (b). A liquid hemisphere forms at the bottom of the upper tube, then a droplet forms and is dragged by the gravity. After the impact of gravity exceeds that of surface tension, the liquid neck breaks and the droplets go into free fall. And subsequently, 1–2 secondary droplets separated from the liquid neck fall down following the main droplet and the rest of liquid neck retracts (sometimes, a string of satellite droplets forms when liquid neck retracting). In short, the droplet development process performs as "Grow-Stretch-Break" if the tube spacing is large enough.

When the tube spacing is relatively small, the liquid may reach the lower tube at the stage of "Stretch," which also shows as "Grow-Stretch-Break," but the sphere droplet cannot be observed. Furthermore, the phenomenon that the liquid touches the lower tube at the stage of "Grow" is discussed in Section 4.2.

It is also found that the dry patch occurs on the tube surface with lower Re (in present experiment, the dry patch appears when Re < 70). The droplets fall from discontinuous droplet departure point, as shown in Fig. 6(a). As Re increases, the droplets tend to fall in synchronization, and then unstable liquid column may appear temporarily due to the transient adhesion of liquid neck on thin film around lower tube. Furthermore, the number of departure point is 3 per 100 mm at Re = 60, which is 4 at Re = 90. While the Re > 200, the departure point spacing stabilizes at about 20 mm.

- Droplet-column flow

When the Re is large enough to prevent a liquid neck from retracting and forms a stable column, the flow pattern turns into droplet-column flow. With Re increases, the number of liquid columns becomes more and the break length becomes longer, as shown in Figs. 6(c)–(e).

- Column flow

At the beginning of column flow pattern, the roots of the columns are very stable, as shown in Figs. 6(f) and (g). Slight waggle of liquid column can be observed when Re exceeds 250, as shown in Figs. 6(h) and (i). At the late period of column flow pattern, the roots of the columns become thicker and instable, two adjacent columns may fuse together, as shown in Fig. 7. A transient phenomenon "Liquid Tooth" is shown in red frame of Fig. 7.

The column flow has the following features: a moderate film thickness can guarantee the tube wetted completely and the liquid columns impingement makes film around tube fluctuate continuously.

While the flow pattern is under the beginning of column flow or increasing the tube spacing in column flow, the curvature radius of the liquid column interface varies repeatedly near the liquid column tail, as shown in Fig. 9. This phenomenon is Plateau–Rayleigh Instability in column flow as a harbinger of the transition from column flow to droplet flow. If tube spacing increases or Re decreases further, the liquid column will turn back into droplet flow.

Two effects influence the liquid column in Plateau–Rayleigh Instability [20]: one effect results from the variation of the column diameter (according to Young–Laplace equation, the larger pressure due to the smaller column diameter compels the fluid to flow to larger diameter region, which promotes the column rupture); the other one derives from the variation of the column profile as shown in Fig. 8. Positive pressure and negative pressure caused separately by convex and concave profile helps to make the column profile uniform. But in general, the two effects cannot be offset exactly. The Young–Laplace equation is shown as following:

$$\Delta p = \sigma\left(\frac{1}{r_1} + \frac{1}{r_2}\right) \tag{2}$$

where Δp is the surface pressure difference for microelement, σ is the surface tension, r_1 and r_2 are radii at two perpendicular directions. Apply Eq. (2) into cylinder, r_2 tends to infinity, Eq. (2) thus turns into :

$$\Delta p = \frac{\sigma}{r} \tag{3}$$

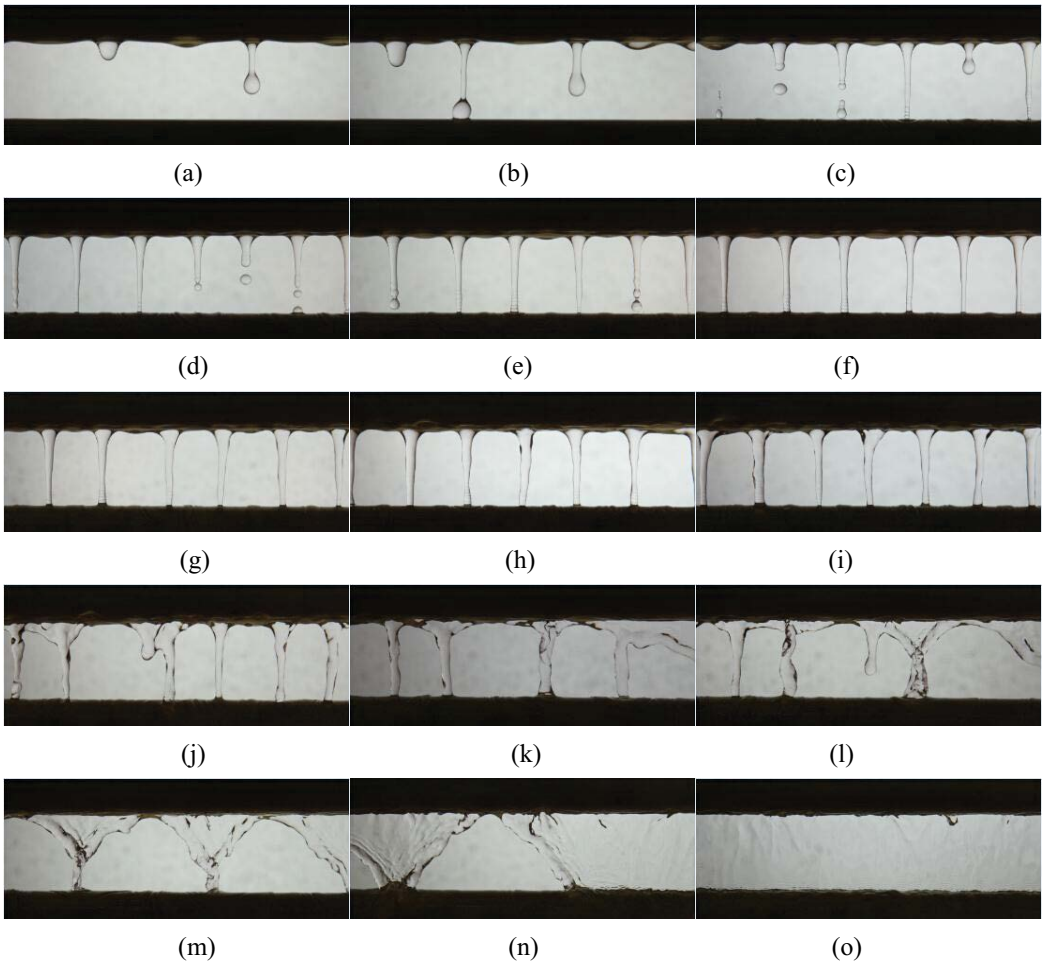

Fig. 6. Flow patterns with d = 19 mm, s = 30 mm. (a) Re = 64.4, (b) Re = 92, (c) Re = 119.6, (d) Re = 138, (e) Re = 165.6, (f) Re = 184, (g) Re = 230, (h) Re = 276, (i) Re = 322, (j) Re = 368, (k) Re = 414, (l) Re = 460, (m) Re = 506, (n) Re = 552, and (o) Re = 598.

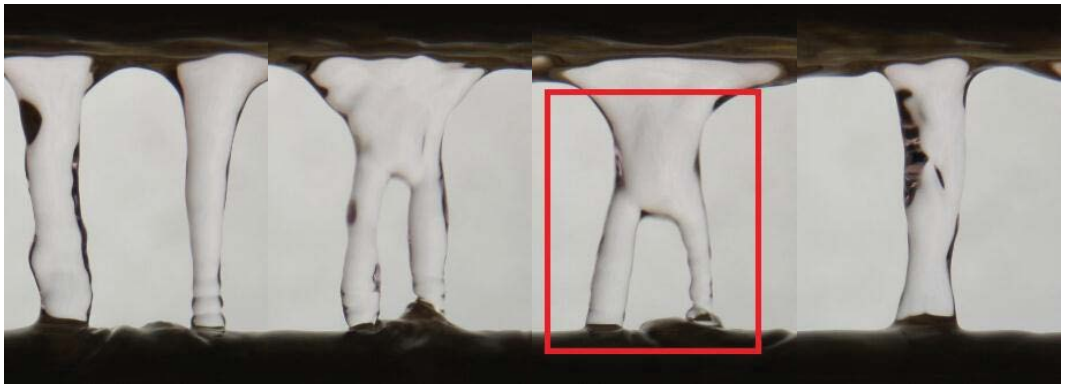

Fig. 7. Process of columns fusion.

where r is radius of liquid column.

- Column-sheet flow

With Re increases, the liquid film around tubes becomes thicker and then the fusion phenomenon appears. At Re = 460, a few columns confuse into liquid sheets with the liquid sheets endings shrinking into columns due to the surface tension so the nascent sheet has a "Y" type, as shown in Fig. 6(l). With the increment of Re, the number of residual columns reduces, the sheet widens and the liquid arch forms.

- Sheet flow

In sheet flow stage, the inconsecutive liquid sheets confuse together with Re increase, as shown in Figs. 6(m)–(o).

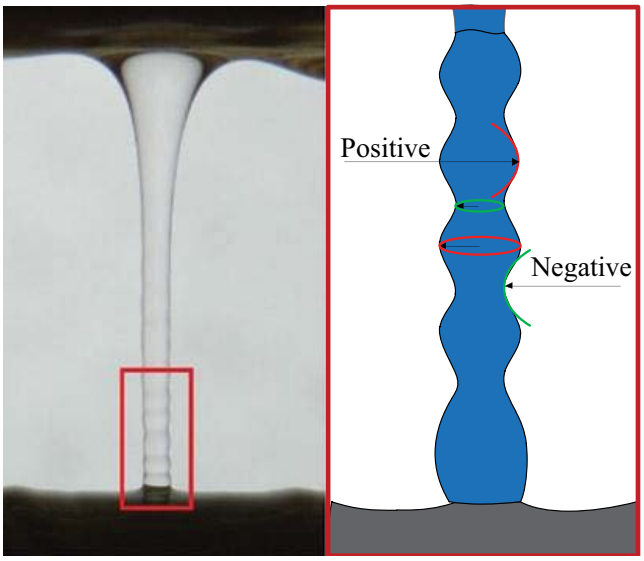

Fig. 8. Plateau–Rayleigh Instability in horizontal inter-tube flow.

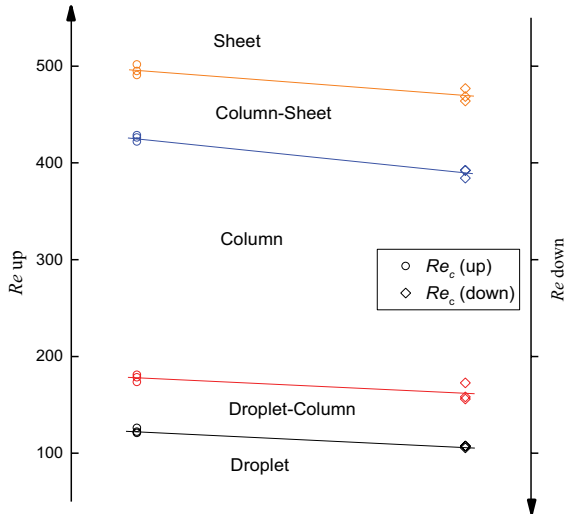

Fig. 9. Hysteresis phenomenon.

At last, a whole liquid sheet forms between tubes. Under sheet flow, the splash is severe and the film thickness is relatively large.

In addition, the in-line column flow does not appear for water due to its small viscosity. The smaller viscosity makes inertia force more dominant, which improves the spreading after the fluid impinges on the tube surface. The overlap forms in the middle of two adjacent columns and the lower liquid column generates underneath the crest. Therefore, only the staggered column flow appears for water in column flow pattern. Even at very small Re, the drops of water droplets are also staggered.

4.1.2. Hysteresis phenomenon

The hysteresis phenomenon was observed with the variation of Re as shown in Fig. 9. The transition from a liquid column to a droplet needs to overcome the cohesive energy for the liquid neck breakage (namely the surface free energy of the two newly generated surfaces). Hence, it is necessary to further decrease Re to reduce the liquid column diameter (comparing with the Re_c from droplet flow to column flow), which can promote to rupture the liquid column according to Young–Laplace equation. Analogously, the transition from column to sheet also needs to overcome the surface free energy of the two new sections produced by breakage of liquid arch. In conclusion, the reason caused the transition hysteresis phenomenon is the "energy difference."

Moreover, it is noted that the hysteresis intervals for column to column-sheet (C/CS) and column-sheet to sheet (CS/S) are larger than that for droplet to droplet-column (D/DC) and droplet-column to column (DC/C). The surface free energy is proportional to the new surface area. The area difference for C/CS and CS/S is the integral of sheet thickness over the tube spacing, but that for D/DC and DC/C is the area of two new sections after the liquid neck breaks. Generally, the former is larger than the latter, hence the hysteresis for transitions C/CS and CS/S are more obvious. This can also explain why Dhir et al. [18], Armbruster and Mitrovic [10] believed the hysteresis only exists in transition from liquid column to sheet.

4.2. Effect of tube spacing

4.2.1. Effect of tube spacing on flow pattern transition

In previous studies, scholars hold different views of the influencing factors in inter-tube flow pattern transitions. Ganić and Roppo [13], Mitrovic [7] suggested that the tube spacing is a significant factor in pattern transitions, but Yung et al. [9,21], Hu and Jacobi [11] believed that the tube spacing has little effect on pattern transitions. It should be noted that all the Re_c increases with the tube spacing at different degrees, as shown in Fig. 10. For example, the Re_c for D/DC and DC/C increase with 8.3% and 8.5% separately with the tube spacing increased from 30 to 5.7 mm, but the increments of Re_c for C/CS and CS/S are more significant with the tube spacing increased from 30 to 5.7 mm, which are 23.3% and 31.6%, respectively. Hence, although the corrections proposed by Hu and Jacobi [11] have a certain guiding significance, the influence of tube spacing cannot be neglected.

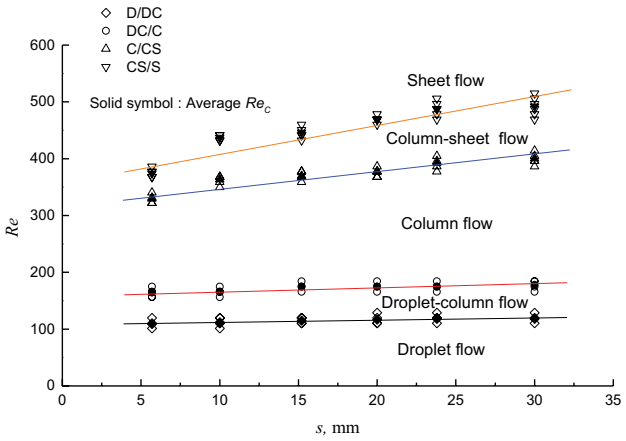

Fig. 10. Re_c for flow pattern transition with d = 19 mm.

The classification for D/DC and DC/C is based on judging the transition between droplet and column. The larger tube spacing results in the larger velocity and smaller diameter of liquid column, which makes the surface free energy for breaking the liquid column smaller, namely it is easier to transit from column to droplet at a larger tube spacing. Similarly, a larger Re_c is required to keep the liquid sheet from separating into liquid columns when it is at a larger spacing.

It is also found that the influence of the tube spacing on C/CS and CS/S is more sensitive than that on D/DC and DC/C. As mentioned in Section 4.1.2, the energy for rupturing the liquid sheet is the integral of sheet thickness over the tube spacing, so that the variation of tube spacing influences the surface free energy more significantly. But for breaking the column, the impact of tube spacing on section area is relatively less.

Fig. 11 shows the inter-tube flow pattern with different tube spacings under the condition of d = 19 mm and Re = 414. It clearly demonstrates an initial column-sheet flow when s = 30 mm, but when s = 15.2 and 10 mm, there are only a few liquid columns exist between tubes and the rest space is full of liquid sheet. While s = 5.7 mm, the inter-tube flow pattern is a completed liquid sheet.

4.2.2. Special phenomenon with undersize tube spacing

Generally, the droplet flow experiences three stages "Grow-Stretch-Break" between tubes. But in particular, the droplet touches the lower tube surface in "Grow" stage and then drains away rapidly when s = 5.7mm with Re below about 90. Consequently, the process of droplet flow only has two stages: "Grow-Break," showing as an incomplete droplet flow (see Fig. 12).

With Re varies from 90 to 160, a new type flow pattern, pseudo-column flow, appears with the characteristics of periodic variation between tubes, as shown in Fig. 13. That is because the Re is not large enough to maintain the stable liquid column. If increases the tube spacing at constant Re, the pseudo-column flow will convert into normal droplet flow. Due to periodicity, the pseudo-column flow is classified in droplet flow.

4.2.3. Hysteresis phenomenon

It is found that the hysteresis not only exists during the Re variation, but also appears in change of tube spacing, especially the transition from inconsecutive liquid sheet to complete sheet. For example, adjust the spray density to a certain value for keeping complete sheet near the critical point at s = 20 mm, and then increase the tube spacing till the liquid sheet breaks. However, when the tube spacing decreases to 20 mm again, the liquid sheet does not fuse together as before. It is needed to further decrease the tube spacing to reduce the superficial area of liquid sheet till it becomes less than the area of the original consecutive liquid sheets, then the inconsecutive liquid sheets can be fused together.

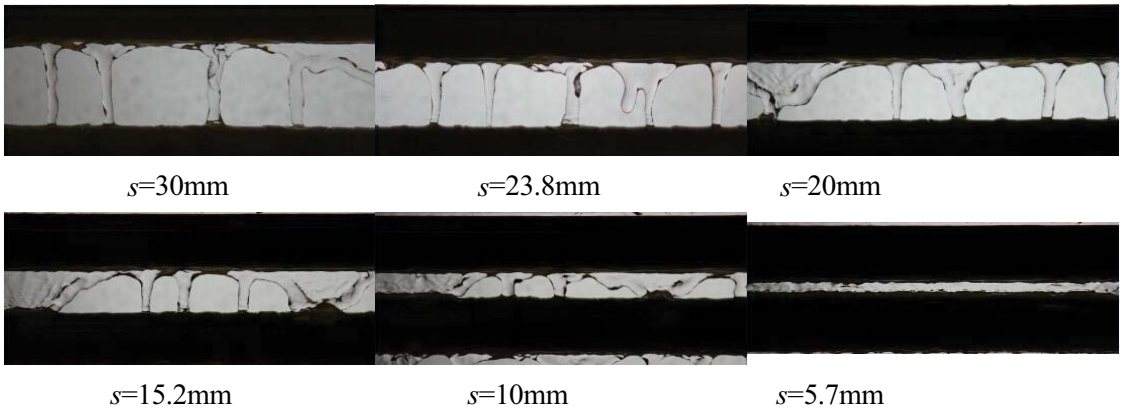

Fig. 11. Flow pattern with different tube spacings.

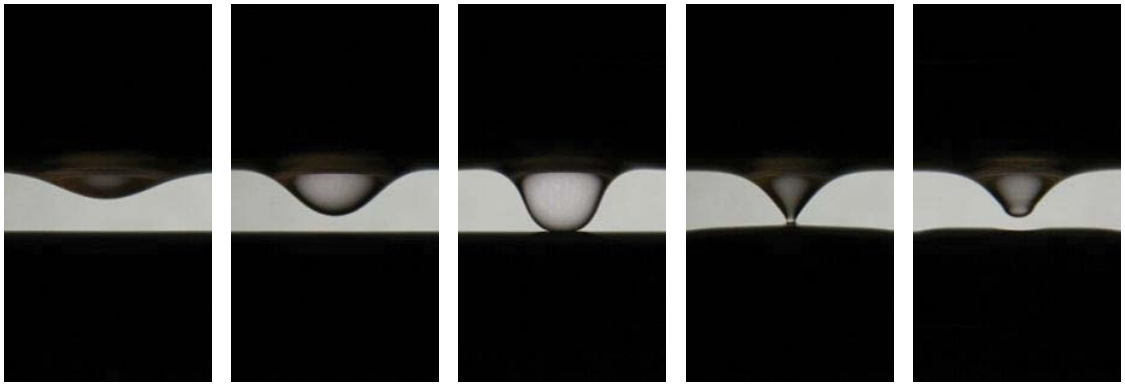

Fig. 12. Incomplete droplet flow.

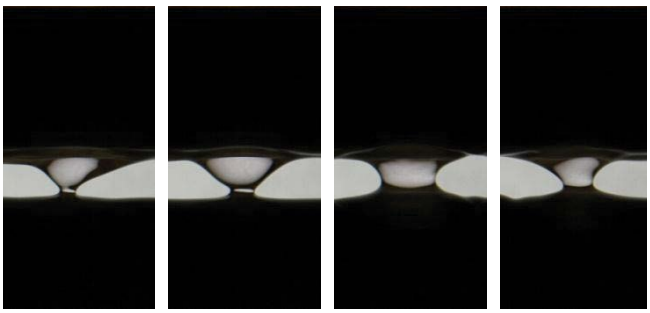

Fig. 13. Pseudo-column flow.

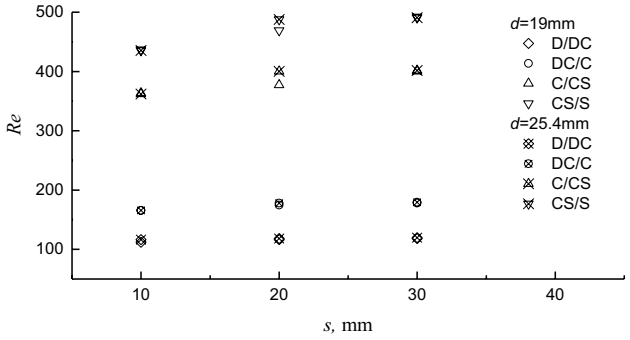

Fig. 14. Re_c for flow pattern transition of d = 19 and 25.4 mm.

4.3. Effect of tube diameter

Fig. 14 shows the comparisons of Re_c between d = 19 and 25.4 mm. It indicates that the tube diameter has little effect on flow pattern transition. Moreover, there is no obvious difference of flow states between them in this experiment.

The diameter variation changes the tube wall curvature and influences the stability and velocity of liquid film around the tube, which indirectly impacts on the accumulation, formation and drop at the tube bottom. But the difference is not significant between 19 and 25.4 mm diameter tubes.

5. Conclusions

An observation experiment was performed to investigate flow patterns and critical transition Reynolds number with the conclusions obtained as following:

- Typically, with Re increases, the flow pattern exhibits in sequence as droplet flow, droplet-column flow, column flow, column-sheet flow, and sheet flow.
- The hysteresis phenomenon exists with the Re variation. The hysteresis intervals for CS/S and C/CS are slightly larger than that for D/DC and DC/C.
- The Re_c increases slightly with tube spacing and the transition for C/CS and CS/S is more sensitive than that for D/DC and DC/C.
- The droplet flow with undersize tube spacing displays as incomplete droplet flow and pseudo-column flow.
- The tube diameter has little effect on flow state and pattern transition under the operating condition selected in this paper.

Symbols

Re	—	Reynolds number
Re_c	—	Critical transition for flow pattern transition
D	—	Droplet flow
DC	—	Droplet-column flow
C	—	Column flow
CS	—	Column-sheet flow
S	—	Sheet flow
d	—	Tube diameter, mm
r	—	Radium for liquid column, mm
p	—	Pressure, N
s	—	Tube spacing, mm
Γ	—	Spray density, kg/(m s)
σ	—	Surface tension, N
μ	—	Dynamic viscosity, Pa S

Acknowledgment

The authors acknowledge the support from National Natural Science Foundation of China (no. 51706011 and no. 51336001).

References

[1] G. Ribatski, A.M. Jacobi, Falling-film evaporation on horizontal tubes – a critical review, Int. J. Refrig., 28 (2005) 635–653.
[2] X. Chen, S.Q. Shen, Y.X. Wang, J.X. Chen, J.S. Zhang, Measurement on thickness distribution of falling film around horizontal tube with laser-induced fluorescence technology, Int. J. Heat Mass Transfer, 89 (2015) 707–713.
[3] H. Hou, Q.C. Bi, H. Ma, G. Wu. Distribution characteristics of falling film thickness around a horizontal tube, Desalination, 285 (2012) 393–398.
[4] D. Gstoehl, J.F. Roques, P. Crisinel, J.R. Thome, Measurement of falling film thickness around a horizontal tube using a laser measurement technique, Heat Transfer Eng., 25 (2004) 28–34.
[5] M. Li, Y. Lu, S. Zhang, Y. Xiao, A numerical study of effects of counter-current gas flow rate on local hydrodynamic characteristics of falling films over horizontal tubes, Desalination, 383 (2016) 68–80.
[6] S.Q. Shen, X. Chen, X.S. Mu, Y.X. Wang, L.Y. Gong, Heat transfer characteristics of horizontal tube falling film evaporation for desalination, Desal. Wat. Treat., 55 (2015) 3343–3349.
[7] J. Mitrovic, Influence of Tube Spacing and Flow Rate on Heat Transfer from a Horizontal Tube to a Falling Liquid Film, Proceedings of the 8th International Heat Transfer, San Francisco, 1986, pp. 1949–1956.
[8] J.T. Rogers, S.S. Goindi, M. Lamari, Turbulent Falling Film Flow and Heat Transfer on Horizontal Tube, Proceedings of the National Heat Transfer Conference, Portland, 1995, pp. 3–12.
[9] D. Yung, J.J. Lorenz, E.N. Ganić, Vapor/liquid interaction and entrainment in falling film evaporators, J. Heat Transfer, 102 (1980) 20–25.
[10] R. Armbruster, J. Mitrovic, Patterns of Falling Film Flow over Horizontal Smooth Tubes, Proceedings of the 10th International Heat Transfer, Brighton, 1994, pp. 275–280.
[11] X. Hu, A.M. Jacobi, The intertube falling film. Part 1. Flow characteristics, mode transitions, and hysteresis, J. Heat Transfer, 118 (1996) 616–625.
[12] Y. Fujita, M. Tsutsui, Evaporation heat transfer of falling films on horizontal tube. Part 2. Experimental study, Heat Transfer Jpn. Res., 24 (1995) 13–31.
[13] E.N. Ganić, M.N. Roppo, An experimental study of falling liquid film breakdown on a horizontal cylinder during heat transfer, J. Heat Transfer, 102 (1980) 342–346.

[14] J.D. Killion, S. Garimella, Gravity-driven flow of liquid films and droplets in horizontal tube banks, Int. J. Refrig., 26 (2003) 516–526.
[15] J.D. Killion, S. Garimella, Pendant droplet motion for absorption on horizontal tube banks, Int. J. Heat Mass Transfer, 47 (2004) 4403–4414.
[16] J.F. Roques, V. Dupont, J.R. Thome, Falling film transitions on plain and enhanced tube, J. Heat Transfer, 124 (2002) 491–499.
[17] J.D. Chen, R.H. Zhang, R.P. Niu, Numerical simulation of horizontal tube bundle falling film flow pattern transformation, Renewable Energy, 73 (2015) 62–68.
[18] V. Dhir, K. Taghavi-Tafreshi, Hydrodynamic Transition During Dripping of a Liquid from Underside of a Horizontal Tube, ASME Paper, 1981, No 81-NWA/H.
[19] B.L. Ruan, A.M. Jacobi, L.S. Li, Vapor Shear Effects on Falling-Film Mode Transitions Between Horizontal Tubes, International Refrigeration and Air Conditioning Conference, Purdue, 2008, 2276, pp. 1–8.
[20] P. Gennes, F. Brochard-Wyart, D. Quéré, A. Reisinger, B. Widom, Capillary and Wetting Phenomena – Drops, Bubbles, Pearls, Waves, Springer, New York, 2004.
[21] D. Yung, J.J. Lorenz, E.N. Ganić, Vapor/Liquid Interaction and Entrainment in Shell-and-Tube Evaporators, ANL-OTEC-78-2, 1978.